

A Joint Delay-Energy-Security Aware Framework for Intelligent Task Scheduling in Satellite-Terrestrial Edge Computing Network

YUHAO ZHENG¹ (*Graduate Student Member, IEEE*), TING YOU² (*Student Member, IEEE*), KEJIA PENG^{3, 4}, AND CHANG LIU²

¹School of Information and Communication Engineering, Beijing University of Posts and Telecommunications, Beijing 100876, China

²Beijing Sport University, Beijing 100084, China

³Nanjing University of Science and Technology, Nanjing 210094, China

⁴Mendeleev University of Chemical Technology of Russia, Moscow 125047, Russia

CORRESPONDING AUTHOR: T. YOU, C. LIU (e-mail: t.you@bsu.edu.cn; c.liu@bsu.edu.cn).

ABSTRACT In this paper, we propose a two-stage optimization framework for secure task scheduling in satellite-terrestrial edge computing networks (STECNs). The framework jointly considers secure user association and task offloading to balance transmission delay, energy consumption, and physical-layer security. To address the inherent complexity, we decouple the problem into two stages. In the first stage, a secrecy-aware user association strategy is designed by discretizing artificial noise (AN) power ratios and identifying feasible links that satisfy secrecy constraints, resulting in a set of candidate secure associations. In the second stage, we formulate a delay-energy-aware task scheduling problem as an integer linear program and solve it using a heuristic Mayfly Algorithm (MA) to obtain low-complexity, high-quality solutions. Extensive simulation results demonstrate the effectiveness and superiority of the proposed framework in achieving secure and efficient task scheduling under dynamic satellite environments.

INDEX TERMS Satellite-terrestrial edge computing network, two-stage framework, secure task scheduling, atomic search optimization.

I. INTRODUCTION

A. BACKGROUND

WITH the rapid development of sixth-generation (6G) networks and satellite communications, the demand for seamless global connectivity and ubiquitous computing services has surged dramatically [1]. As terrestrial infrastructures alone cannot fulfill such demand, especially in remote, oceanic, or emergency areas, the concept of satellite-terrestrial network (STN) has been proposed. STN tightly integrate low Earth orbit (LEO) satellites and ground infrastructures to achieve wide-area coverage and service availability [2]. Meanwhile, mobile edge computing (MEC) has emerged as a key enabler of low-latency and computation-intensive services by bringing computational capabilities closer to end users [3]. By combining the global coverage of STN with the distributed computing ability of MEC, satellite-terrestrial edge computing network (STECN) have become a promising architecture to support intelligent task scheduling with strong spatiotemporal flexibility [4].

In recent years, STECN have received increasing attention, aiming to improve computational responsiveness, real-time task processing, and overall network efficiency. Existing studies have explored various technological aspects of STECN, including network slicing [5], resource allocation [6], task offloading [7], and edge server selection [8]. These works have made significant progress in addressing key performance metrics such as end-to-end latency, resource utilization, and energy consumption. However, most existing research assumes a trusted or closed network environment, paying little attention to the critical issue of secure transmission, which is especially crucial in the open and dynamic space-ground scenario [9]. The broadcast nature of satellite links, combined with increasing threats from passive or active adversaries, makes task data highly vulnerable to eavesdropping and interception. This challenge is particularly significant in mission-critical and privacy-sensitive application scenarios, such as military surveillance, emergency response, remote medical diagnosis, and confidential indus-

trial operations [10], where user tasks may contain sensitive information and privacy-critical models. In such contexts, ignoring security considerations in task scheduling may lead to severe privacy leakage or mission failure. Therefore, STECN must support secure task offloading and association, which not only satisfies traditional performance goals but also meets physical-layer secrecy constraints. Secure task scheduling under secrecy capacity limitations remains largely unexplored in the STECN context.

Beyond the challenge of secure transmission, STECN faces a multitude of unique constraints that significantly complicate the task scheduling process. First, LEO satellites are characterized by rapid orbital movement, which leads to highly dynamic and time-varying network topologies. This results in frequent handovers, rapidly changing link quality, and intermittent satellite visibility for ground users [11]. Second, due to limitations in payload capacity and power supply, each satellite is equipped with only a modest amount of computational and energy resources [12]. These limitations severely restrict the number of tasks a satellite can process and limit the computational intensity of the services it can support. Third, task scheduling in STECN must be optimized not only across space but also across time, while taking into account varying channel conditions and the presence of eavesdroppers. This spatiotemporal complexity is further compounded by dynamic security threats, where myopic scheduling focused only on delay or energy may increase exposure to risks or cause future resource bottlenecks.

B. RELATED WORKS

Recent years have witnessed growing interest in STECN, which provides low-latency and computation-intensive services in a broader coverage area [4]. A variety of technological dimensions have been explored in this context. For example, Gao *et al.* in [8] employed a hybrid approach combining K-center clustering and NSGA-II to reduce latency and energy consumption in STECN environments. Esmat *et al.* in [5] investigated resilient network slicing techniques tailored for satellite edge computing (SEC), emphasizing service continuity through dynamic management and orchestration. Furthermore, Wei *et al.* in [7] addressed joint slicing and offloading through a bi-level game model and distributed solution design, while Esmat *et al.* in [13] proposed a cross-domain slicing mechanism based on restless multi-armed bandit (RMAB) processes for satellite-ground resource coordination. While these studies have provided valuable insights into resource allocation, task offloading, and service orchestration in STECN, they primarily focus on performance optimization under trusted environments, overlooking critical security issues in open and dynamic space-ground systems. In particular, physical-layer security in task transmission and scheduling has not been systematically addressed.

Although most existing studies on MEC and edge computing focus on performance metrics such as latency or energy efficiency, only a limited number of works have explored

secure task scheduling and computation offloading under adversarial threats. For instance, Wu *et al.* [14] proposed a cooperative jamming-assisted computation offloading scheme that jointly optimizes service caching, transmit power, and offloading decisions to minimize delay in the presence of eavesdropping threats. Zhou *et al.* [15] designed a secure computation offloading framework for cache-assisted ultra-dense MEC networks, which minimizes energy consumption under strict delay, resource, and security constraints. Similarly, Zahed *et al.* [16] developed a green and secure MEC architecture for IoT applications, integrating edge caching, cooperative task offloading, and security service assignment to reduce both energy and potential security breach costs. While these works address security-aware task scheduling in terrestrial MEC networks, there is a notable absence of research focusing on secure task scheduling in satellite network. Given the unique challenges of STECN environment, developing a comprehensive and secure task scheduling framework for STECN is both necessary and urgent.

C. CONTRIBUTIONS

We propose a two-stage delay-energy-security aware scheduling framework, aiming to achieve secure, low-latency, and energy-efficient task scheduling under dynamic satellite topologies and constrained resources. The proposed framework integrates a secure user association mechanism and an efficient task scheduling strategy. At the first stage, we formulate a secure association strategy under secrecy capacity constraints to protect users from eavesdropping threats. At the second stage, we develop a delay-energy-aware task scheduler based on Mayfly algorithm (MA), enabling task scheduling under time-varying environment. The main contributions are summarized as follows:

- We design the system architecture of STECN and detail the secure scheduling process. A two stage framework is developed to accurately capture dynamic states of LEO satellites and user requests across different time slots.
- At the first stage, we formulate the user association problem under secrecy capacity constraints, and develop a secure association strategy that dynamically selects LEO satellites to ensure privacy-preserving and adaptive user access in dynamic topologies.
- At the second stage, we focus on task scheduling under delay-energy performance. GA algorithm is designed to efficiently schedule tasks among satellites, minimizing delay and energy consumption while adapting to resource fluctuations and link variability.
- Extensive simulations validate the proposed framework under practical LEO dynamics, demonstrating its effectiveness in reducing task delay and energy consumption while ensuring secure service delivery, compared with baseline approaches.

II. SYSTEM DESCRIPTION

In this section, we first describe our system model in our research.

A. NETWORK MODEL

We consider a LEO satellite network that supports secure task scheduling from LEO satellites to legitimate users. Let $\mathcal{N} = \{1, \dots, N\}$ denote the set of LEO satellites, and $\mathcal{U} = \{1, \dots, U\}$ denote the set of legitimate users. Each LEO satellite $n \in \mathcal{N}$ can perform computational service for users. The eavesdroppers can be denoted as $\mathcal{E} = \{1, \dots, E\}$. We assume that the LEO satellite network has secure inter-satellite links (ISLs), which enable data exchange between LEO satellites without risk of eavesdropping. Due to the highly dynamic and periodic nature of LEO satellites, the system operates in discrete time slots indexed by $t \in \mathcal{T} = \{1, 2, \dots, T\}$. Due to constrained computing resources on-board, each LEO satellite can execute a limited number of tasks. Let $\mathcal{R}(t) = \{r_1(t), \dots, r_U(t)\}$ be the set of all user task requests. Task scheduling decision can be denoted by binary variable $o_{n,u}(t) \in \{0, 1\}$, where $o_{n,u}(t) = 1$ indicates that LEO satellite n execute task r_u in time t , and 0 otherwise. The computational requirements of task $r_u(t)$ is denoted as c_u .

Due to the limited beam coverage of LEO satellites, user association is constrained by the beamwidth. Let θ_{beam} be the half beamwidth angle of the LEO satellite, and $\theta_{n,u}(t)$ denote the central angle between the LEO satellite n and the user u in time t . User u can be associated with LEO satellite n only if it lies within the beam coverage region of the LEO satellite. The upper bound of the central angle can be mathematically expressed as [17]:

$$\theta_{\max} = \begin{cases} \sin^{-1}\left(\frac{R_n}{R_0} \sin \theta_{\text{beam}}\right) - \theta_{\text{beam}}, & \theta_{\text{beam}} < \sin^{-1}\left(\frac{R_0}{R_n}\right) \\ \cos^{-1}\left(\frac{R_0}{R_n}\right), & \theta_{\text{beam}} \geq \sin^{-1}\left(\frac{R_0}{R_n}\right) \end{cases} \quad (1)$$

where R_0, R_n are the radius of the earth and LEO satellites. Let $\Psi_u(t)$ denotes the available set of LEO satellites whose $\theta_{n,u}(t)$ is in the range $[0, \theta_{\max}]$ for user u . The user chooses the LEO satellite in $\Psi_u(t)$ to be the association LEO satellite n_0 . We define $a_{n,u}(t) \in \{0, 1\}$ to represent the association decision of user u . When user u is directly associated with LEO satellite n in time t , $a_{n,u}(t) = 1$; otherwise, $a_{n,u}(t) = 0$.

B. SECURE COMMUNICATION MODEL

We incorporate artificial noise and both large-scale and small-scale fading to characterize the communication model.

1) Artificial Noise

In this article, we introduce AN into the transmitted signal to enhance its secrecy. Our goal is to ensure that legitimate users can correctly receive the transmitted data, while eavesdroppers cannot successfully decode the information. Let P_t be the total transmit power allocated by the satellite, which is divided

between the useful signal and the AN. Let ψ denote the information-bearing ratio, which falls within the interval $[0, 1]$. Then the power for the signal is ψP_t , and the power for AN is $(1 - \psi)P_t$.

2) Downlink Model

We model satellite-to-ground wireless channel. Large-scale fading is primarily modeled by the free-space path loss. The large-scale path loss between LEO satellite n and user u is given by:

$$L_{n,u}(t) = \left(\frac{c}{4\pi f_c d_{n,u}(t)} \right)^2 \quad (2)$$

where c is the speed of light, f_c is the carrier frequency, and $d_{n,u}(t)$ denotes the distance between LEO satellite n and user u . We adopt the Shadowed-Rician (SR) fading model, which is widely used for satellite-ground communication [18]. The small scale fading coefficient is denoted as $|h_{n,u}(t)|^2$, where $h_{n,u}(t)$ is a complex random variable governed by the SR distribution. Combining the effects of large-scale path loss and small-scale fading, the received signal power at user u from LEO satellite n is given by:

$$P_{n,u}^{\text{rec}}(t) = P_t \cdot G \cdot L_{n,u}(t) \cdot |h_{n,u}(t)|^2 \quad (3)$$

where G represents the combined antenna gain of the LEO satellite transmitter and ground receiver. Then, the signal-to-interference and noise ratio (SINR) at the legitimate user can be given by:

$$\text{SINR}_{n_0,u}(t) = \frac{\psi P_{n_0,u}^{\text{rec}}(t)}{\sum_{n \in \{\Psi_u/n_0\}} P_{n,u}^{\text{rec}}(t) + \sigma^2}, \quad (4)$$

where σ^2 is the noise power. The corresponding downlink transmission rates for the legitimate user can be expressed as:

$$R_{n_0,u}(t) = W_0 \log_2(1 + \text{SINR}_{n_0,u}(t)) \quad (5)$$

where W_0 is the available LEO satellite bandwidth. Similarly, the SINR at the eavesdropper can be given by:

$$\text{SINR}_{n_0,e}(t) = \frac{\psi P_{n_0,e}^{\text{rec}}(t)}{(1 - \psi) P_{n_0,e}^{\text{rec}}(t) + \sum_{n \in \{\Psi_e/n_0\}} P_{n,e}^{\text{rec}}(t) + \sigma^2} \quad (6)$$

The corresponding downlink transmission rates for the eavesdropper can be expressed as:

$$R_{n_0,e}(t) = W_0 \log_2(1 + \text{SINR}_{n_0,e}(t)) \quad (7)$$

Increasing the artificial noise power can effectively suppress $\text{SINR}_{n_0,e}(t)$ and $R_{n_0,e}(t)$, but it may also degrade $\text{SINR}_{n_0,u}(t)$ and reduce $R_{n_0,u}(t)$. Conversely, allocating more power to the useful signal improves $R_{n_0,u}(t)$ but also increases $R_{n_0,e}(t)$. Therefore, there exists a tradeoff in power allocation that needs to be carefully optimized. On this basis, the secrecy transmission rate, which is defined as the difference of the achievable rate between the legitimate transmission rate and the eavesdropping transmission rate is given by:

$$R_{n_0,u}^{\text{sec}}(t) = \left[R_{n_0,u}(t) - \max_{e \in \mathcal{E}} R_{n_0,e}(t) \right]^+ \quad (8)$$

where $[x]^+$ is defined as $\max\{0, x\}$.

3) Inter-Satellite Link Model

LEO satellites use lasers to achieve ISL interconnection. The relative positions of LEO satellites within the same orbital plane remain stable, and stable inter-orbital distances enable connections with nearby LEO satellites in adjacent planes [19]. With four inter-satellite links (ISLs), LEO satellites form a grid topology orbital network. The data transmission rate from adjacent LEO satellite n to m in time slot t can be represented as [20]:

$$R_{n,m}^S(t) = \frac{P_n G_n^{TX} G_m^{RX} L_{n,m}(t)}{b T_s \cdot \left(\frac{E_b}{N_0} \right) \cdot M}, \quad (9)$$

where $L_{n,m}(t)$ is the free space loss between LEO satellite n and m in time slot t . b is the Boltzmann constant, T_s is the total system noise temperature, $\left(\frac{E_b}{N_0} \right)$ is the required received energy per bit relative to noise density, M is the link margin. Due to we do not regard LEO satellites as eavesdroppers, we assume the ISLs are secure during data transmission. To mitigate interference from multiple requests on the wireless channels, we use Orthogonal Frequency Division Multiplexing (OFDM) to assign a unique subchannel for each request and equally divide the total bandwidth among all subchannels. This ensures orthogonality and prevents interference between the subcarriers.

C. DELAY MODEL

The average delay comprises the data transmission delay, the waiting delay at the data buffer, and the execution delay. The data transmission delay is determined by data size and achievable transmission rate. Let $\zeta_u(t)$ denote the size of the result data of task $r_u(t)$, then the data transmission delay is:

$$D_{u,n}^{\text{trans},m}(t) = \frac{\zeta_u(t)}{R_u(t)} + \sum_{p,q \in e_{n_0,m}(t)} \frac{o_{m,u}(t) \zeta_u(t)}{R_{p,q}(t)} \quad (10)$$

where $e_{n_0,m}(t)$ is the transmission path in the ISL. We employ the Floyd algorithm to determine the transmission path $e_{n_0,m}(t)$. If the task is scheduled to LEO satellite m , the data transmission delay comprises the downlink transmission delay of association LEO satellite n_0 , and the ISL transmission delay from LEO satellite m to n_0 (if exists).

The tasks execution delay is predominantly linked to the computing resources needed for the task and the computing capacities of the LEO satellites. The execution delay can be computed as follows:

$$D_{u,n}^{\text{comp},m} = \frac{o_{m,u}(t) \zeta_u(t) c_u(t)}{f_m} \quad (11)$$

where f_m denotes the computing resources (CPU cycles per second) of the LEO satellite m .

When request $r_u(t)$ arrives at the data queue of satellite m , the computing task needs to wait for processing. We assume that $Q_{m,u}(t)$ represents the collection of requests prior to request $r_u(t)$ in the queue of LEO satellite m at time t . Once all the previous content requests of $r_u(t)$ have been processed, $r_u(t)$ will be processed at LEO satellite m . The waiting time

of the task is determined by the execution time of all existing computing tasks in the queue. The queuing delay caused by the previously accumulated tasks for request $r_u(t)$ can be expressed as:

$$D_{u,n}^{\text{queue},m}(t) = \sum_{r_d(t) \in Q_{v,u}(t)} \frac{o_{m,d}(t) \zeta_d(t) c_d(t)}{f_m}, \quad (12)$$

where $r_d(t)$ represents a task request in the previous request queue $Q_{v,u}(t)$, $o_{m,d}(t)$ denotes the scheduling decision for task request $r_d(t)$, $\zeta_d(t)$ indicates the data size of task request $r_d(t)$, and $c_d(t)$ represents the computational requirements of task request $r_d(t)$. Then, the average delay is thus given by:

$$D_{u,n}(t) = \sum_{n \in \mathcal{N}} \left(D_{u,n}^{\text{trans},m}(t) + D_{u,n}^{\text{comp},m}(t) + D_{u,n}^{\text{queue},m}(t) \right). \quad (13)$$

D. ENERGY CONSUMPTION MODEL

The energy consumption comprises the energy consumption for transmission and execution. The transmission energy consumption used to transmit task r_u to LEO satellite m can be expressed as follows:

$$E_{n,u}^{\text{trans},m}(t) = P_t D_{u,n}^{\text{trans},m}(t). \quad (14)$$

The execution energy consumption of LEO satellite m for executing task r_u can be given by:

$$E_{n,u}^{\text{comp},m}(t) = \varepsilon(f_m)^3 D_{u,n}^{\text{comp},m}(t), \quad (15)$$

where $\varepsilon(f_m)^3$ is the function of power and computing capability [21]. Then, the average energy consumption is computed as:

$$E_{n,u}(t) = \sum_{m \in \mathcal{N}} \left(E_{n,u}^{\text{trans},m}(t) + E_{n,u}^{\text{comp},m}(t) \right). \quad (16)$$

E. PROBLEM FORMULATION

Our objective is to design an efficient scheduling and user association strategy that jointly minimizes task delay and energy consumption while ensuring a minimum level of communication secrecy. Specifically, we formulate a constrained optimization problem where the goal is to minimize the total system cost composed of delay and energy terms, subject to secrecy rate and resource capacity constraints. The problem is expressed as:

$$(P1) \quad \min_{a_{n,u}, o_{n,u}, \psi} \sum_{t \in \mathcal{T}} \sum_{n \in \mathcal{N}} \sum_{u \in \mathcal{U}} (\kappa^D \cdot D_{n,u}(t) + \kappa^E \cdot E_{n,u}(t)) \quad (17)$$

$$\text{subject to} \quad \begin{cases} \kappa^D + \kappa^E = 1, \\ R_{n_0,u}^{\text{sec}}(t) \geq \epsilon, \quad \forall u \in \mathcal{U}, \\ \psi \in (0, 1), \quad \forall n \in \mathcal{N}. \end{cases} \quad (18)$$

where κ^D, κ^E are performance gain coefficients. In the constraints, we need to ensure that the secrecy offloading rate must exceed the secrecy requirement to ensure secure computation offloading. Meanwhile, the designed AN must fall within the interval $[0, 1]$.

III. PROPOSED TWO-STAGE HEURISTIC ALGORITHM

This section introduces a novel framework to address the problem of secure user association and task scheduling in two stages.

A. PROBLEM ANALYSIS AND DECOMPOSITION

The original optimization problem (P1) jointly considers user association, task scheduling, and AN power configuration to minimize the delay and energy consumption while ensuring secure communication. However, the problem is formulated as a mixed-integer nonlinear program with strong coupling among binary user association decision $a_{n,u}$, task scheduling decision $o_{n,u}$, and continuous AN power ratio ψ . The combination of discrete and continuous variables, dynamic task arrivals, and fluctuating satellite resources makes real-time global optimization intractable for STECN. To address this challenge, we adopt a two-stage decomposition approach that decouples the secure communication structure from the scheduling decision, thereby reducing computational complexity and enabling scalability. Specifically, we decompose the original problem into two sequential subproblems:

- First Stage: Joint AN power allocation and user association. In this stage, we aim to construct a secure communication topology by determining the user-satellite association and AN power ratio that maximize the achievable secrecy rate, under link dynamics and satellite mobility
- Second Stage: Delay-energy-aware task scheduling. Based on the secure associations obtained in first stage, we perform task scheduling under delay and energy constraints, using heuristic search techniques to allocate resources efficiently under satellite computation and bandwidth limitations.

This decomposition allows each subproblem to be handled independently using tailored heuristics, while preserving the overall system objective of secure and efficient task offloading in dynamic STECN environments. The following subsections detail the design and implementation of each stage.

B. FIRST STAGE: JOINT AN POWER ALLOCATION AND USER ASSOCIATION

Achieving strict physical-layer secrecy ($R_{n_0,u}^{\text{sec}} \geq \epsilon$) for all users in STECN is often infeasible due to the randomness of eavesdropper distribution and dynamic link conditions. Simulation results show that enforcing such a hard constraint leads to frequent failure in user association. Therefore, we relax the constraint and instead maximize the number of users meeting the secrecy threshold under varying AN power ratios.

We discretize the AN power allocation ratio ψ into a finite candidate set $\{0, \Delta, 2\Delta, \dots, 1\}$, where Δ is a tunable step size controlling the granularity of the search space. For each candidate ψ , we evaluate the achievable secrecy rate $R_{n,u}^{\text{sec}}(\psi)$ for each user-satellite pair (u, n) , and attempt to find an association such that user u is connected to a satellite $n \in \Phi_u$

Algorithm 1: Joint AN Power Allocation and User Association

Input: LEO satellite set \mathcal{N} , legitimate user set \mathcal{U} , eavesdropper set \mathcal{E} , secrecy rate threshold ϵ

```

1 Initialize  $a^* \leftarrow \emptyset, \psi^* \leftarrow 0, \Gamma_{\max} \leftarrow 0$ ;
2 for each  $\psi \in \{0, \Delta, 2\Delta, \dots, 1\}$  do
3   Initialize  $a \leftarrow \emptyset, \Gamma(\psi) \leftarrow 0$ ;
4   for each user  $u \in \mathcal{U}$  do
5     Initialize  $R_{\max}^{\text{sec}} \leftarrow -\text{inf}, n^* \leftarrow \emptyset$ ;
6     for each available satellite  $n \in \Phi_u$  do
7       Compute user  $R_{n,u}(\psi)$  by Eq.(5);
8       Compute eavesdropper  $R_{n,e}(\psi)$  by Eq.(7);
9       Compute secrecy  $R_{n,u}^{\text{sec}}(\psi)$  by Eq.(8);
10      if  $R_{n,u}^{\text{sec}}(\psi) > R_{\max}^{\text{sec}}$  then
11        Update  $R_{\max}^{\text{sec}} \leftarrow R_{n,u}^{\text{sec}}(\psi), n^* \leftarrow n$ ;
12    Assign  $a_u \leftarrow n^*$ ;
13    if  $R_{\max}^{\text{sec}} \geq \epsilon$  then
14      Increment  $\Gamma(\psi) \leftarrow \Gamma(\psi) + 1$ ;
15  if  $\Gamma(\psi) > \Gamma_{\max}$  then
16    Update  $\Gamma_{\max} \leftarrow \Gamma(\psi), a^* \leftarrow a, \psi^* \leftarrow \psi$ ;

```

Output: Optimal user association a^* , optimal AN power ratio ψ^*

satisfying the secrecy condition:

$$R_{n,u}^{\text{sec}}(\psi) = R_{n,u}(\psi) - \max_{e \in \mathcal{E}} R_{n,e}(\psi) \geq \epsilon, \quad (19)$$

where $R_{n,u}(\psi)$ and $R_{n,e}(\psi)$ denote the achievable rates of the legitimate user and the strongest eavesdropper, respectively. We define the reliable transmission rate (RTP) under a given AN power ratio ψ as the proportion of users that can be securely served:

$$\Gamma(\psi) = \frac{1}{U} \sum_{u \in \mathcal{U}} \mathbb{D} \{ \exists n \in \Phi_u : R_{n,u}^{\text{sec}}(\psi) \geq \epsilon \}, \quad (20)$$

where $\mathbb{D}\{\cdot\}$ is the indicator function. Our optimization objective at this stage becomes:

$$(P2) \quad (\psi^*, a^*) = \arg \max_{\psi, a} \Gamma(\psi), \quad (21)$$

where $a = \{a_u\}_{u \in \mathcal{U}}$ denotes the user association decision. By jointly searching over ψ and user associations a , we construct a secure communication topology that is most effective under the current conditions.

Algorithm 1 outlines the detailed process. For each candidate ψ , we greedily associate users to satellites offering the highest achievable secrecy rates and record the secure association count $\Gamma(\psi)$. If the current configuration yields a higher count than previous attempts, the algorithm updates the optimal pair (ψ^*, a^*) . This stage thus produces both the optimal AN configuration and the corresponding secure association strategy, which are passed to the next stage for delay-energy-aware task scheduling.

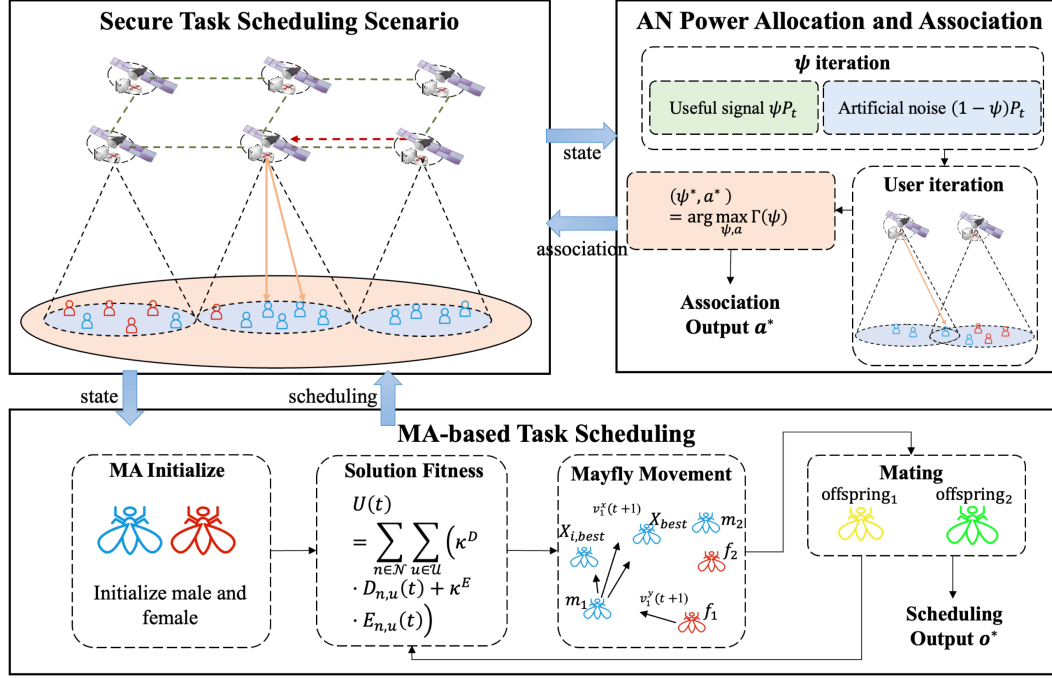


FIGURE 1. Task scheduling performance of different schemes.

C. SECOND STAGE: MA-BASED DELAY-ENERGY-AWARE TASK SCHEDULING

After determining the secure user association and AN power ratio in the first stage, we proceed to optimize the task scheduling strategy. In this stage, each individual mayfly encodes a candidate offloading decision $o = \{o_{n,u}\}_{n \in \mathcal{N}, u \in \mathcal{U}}$, where $o_{n,u} = 1$ indicates that user task is assigned to satellite n . The goal is to minimize a weighted sum of delay and energy consumption across all users:

$$(P3) \quad \min_o \sum_{n \in \mathcal{N}} \sum_{u \in \mathcal{U}} (\kappa^D \cdot D_{n,u} + \kappa^E \cdot E_{n,u}), \quad (22)$$

where $\kappa^D + \kappa^E = 1$, controlling the balance between delay and energy concerns. Given the combinatorial nature of the binary scheduling variables and resource coupling across satellites, this problem is NP-hard and difficult to solve exactly in real time. To this end, we adopt the bio-inspired Mayfly Algorithm (MA) [22] to efficiently explore the solution space. Compared with traditional heuristics, MA incorporates both swarm-based movement (via velocity-position updates) and evolutionary mating, which improves convergence speed and avoids premature stagnation.

By modeling each scheduling strategy as a mayfly individual, we iteratively evolve the population through attraction-based movement, nuptial dance adjustment, and mating crossover. This enables the framework to adaptively balance global search and local refinement. The full MA-based scheduling procedure is described below.

• *Initialization of Candidate Solutions:* We define the male and female populations for task scheduling as:

$$X = [X^1, \dots, X^I]^T, \quad Y = [Y^1, \dots, Y^I]^T, \quad (23)$$

Algorithm 2: MA-based Delay-Energy-Aware Task Scheduling Algorithm

Input: Task set \mathcal{T} , available LEO satellites \mathcal{N} , secure association vector a^* , system parameters

- 1 Initialize MA parameters; randomly initialize male and female mayfly populations X, Y , and their velocities v ;
- 2 **for** iteration = 1 to $Iter_{max}$ **do**
- 3 **for** each male mayfly $X_i \in X$ **do**
- 4 Compute fitness value $Fit_i(t)$ based on Eq. (22) (delay-energy cost function);
- 5 Update global best fitness $Fit_{best}^x(t)$ and individual best $Fit_{i,best}^x(t)$;
- 6 Update position and velocity using Eq. (26) and Eq. (27);
- 7 Perform nuptial dance update using Eq. (28) if X_i is global best;
- 8 **for** each female mayfly $Y_i \in Y$ **do**
- 9 Update position and velocity using Eq. (29) and Eq. (30);
- 10 Perform mating crossover using Eq. (32) to generate offspring;

Output: Optimized task scheduling decision o^*

where X denotes the male mayfly population, Y denotes the female mayfly population. The number of male and female is the same. The initial positions and velocities are randomly initialized.

• *Fitness Evaluation*: Each individual's fitness is computed based on the objective function in Eq. (22), producing:

$$\text{Fit}^x = [\text{Fit}_1^x, \dots, \text{Fit}_I^x], \quad \text{Fit}^y = [\text{Fit}_1^y, \dots, \text{Fit}_I^y]. \quad (24)$$

We define the global best fitness among males as:

$$\text{Fit}_{\text{best}}^x(t) = \min_i \text{Fit}_i^x(t), \quad (25)$$

where $\text{Fit}_i^x(t)$ is the fitness value of male mayfly i at time t . Let $x_{i,\text{best}}$ denote the position of historical best fitness value $\text{Fit}_{i,\text{best}}^x(t)$ of male individual X_i . Let x_{best} denote the global best position of male individuals.

• *Male Mayfly Movement*: Male mayflies gather in swarms, and their position updates are influenced by neighboring individuals. The position update of each male mayfly is given by:

$$x_i(t+1) = x_i(t) + v_i(t+1), \quad (26)$$

where the velocity update follows:

$$\begin{aligned} v_i^d(t+1) = & v_i^d(t) + a_1 e^{-\beta r_p^2} (x_{i,\text{best}}^d - x_i^d) \\ & + a_2 e^{-\beta r_g^2} (x_{\text{best}}^d - x_i^d). \end{aligned} \quad (27)$$

where a_1 and a_2 are positive attraction constants, β is the visibility coefficient of the mayfly. r_p and r_g represent the cartesian distances between x_i and both $x_{i,\text{best}}$ and x_{best} , respectively. Additionally, the best males perform a nuptial dance by adding random movement:

$$v_i^d(t+1) = v_i^d(t) + k \cdot r, \quad r \in [-1, 1]. \quad (28)$$

where k is the nuptial dance distance coefficient, and r is a random number in the range $[-1, 1]$.

• *Female Mayfly Movement*: Female mayflies are attracted to males based on fitness and distance, updating position as:

$$y_i(t+1) = y_i(t) + v_i(t+1), \quad (29)$$

and adjusting velocity via:

$$v_i^d(t+1) = \begin{cases} v_i^d(t) + a_2 e^{-\beta r_{mf}^2} (x_i^d - y_i^d), & \text{if } \text{Fit}_i^y > \text{Fit}_i^x, \\ v_i^d(t) + fl \cdot r, & \text{otherwise.} \end{cases} \quad (30)$$

where r_{mf} is the cartesian distance between male and female mayflies. The parameter fl is the random walk coefficient.

• *Mating and Offspring Generation*: Each male-female pair undergoes crossover to produce two offspring:

$$\text{offspring}_1^i = L \cdot X^i + (1 - L) \cdot Y^i, \quad (31)$$

$$\text{offspring}_2^i = (1 - L) \cdot X^i + L \cdot Y^i, \quad (32)$$

where L is a random scalar in $[0, 1]$.

• *Termination and Output*: The algorithm terminates after a maximum number of iterations. The best individual from the final population is returned as the optimal task scheduling decision. The overall procedures is shown in Fig.2.

Algorithm 3: Two-Stage Delay-Energy-Security-Aware Scheduling Framework

Input: Time period \mathcal{T} , legitimate user set \mathcal{U} , LEO satellite set \mathcal{N} , AN ratio set $\{\psi\}$

```

1 for each time slot  $t \in \mathcal{T}$  do
2   Update network topology, channel state, and user
   task arrivals;
   // Stage 1: Secure Association
3   Invoke Algorithm 1 to obtain secure user
   association  $(a_t^*, \psi_t^*)$ ;
   // Stage 2: Task Scheduling
4   Given  $a_t^*$ , invoke Algorithm 2 to compute optimal
   scheduling decision  $o_t^*$ ;
5   Execute  $(a_t^*, o_t^*)$  for time slot  $t$ ;
```

Output: Scheduling and association trajectories
 $\{(a_t^*, o_t^*)\}_{t \in \mathcal{T}}$

D. TWO-STAGE OPTIMIZATION FRAMEWORK

We propose a two-stage heuristic optimization framework to address the delay-energy-security-aware scheduling problem in STECN. In the first stage, the algorithm iteratively searches over a set of discretized AN power ratios and identifies the secure user association strategy that maximizes the number of users meeting the secrecy rate constraint. In the second stage, based on the selected secure association, we apply a mayfly algorithm (MA) to optimize task scheduling decisions with respect to delay and energy consumption. This hierarchical design decouples the security and resource objectives, allowing efficient and scalable optimization in dynamic satellite-edge environments.

The overall complexity of the proposed two-stage framework includes secure user association with AN power allocation and task scheduling via the mayfly algorithm. In the first stage, we evaluate $\frac{1}{\Delta}$ candidate AN ratios, each involving user-to-satellite association with complexity $\mathcal{O}(U)$, resulting in $\mathcal{O}(\frac{1}{\Delta} \cdot U)$. In the second stage, the MA-based scheduler operates on the selected association with complexity $\mathcal{O}(\text{Iter}_{\max} \cdot I)$, where I is the population size and Iter_{\max} is the iteration limit. Therefore, the total computational complexity is $\mathcal{O}(\frac{1}{\Delta} \cdot U + \text{Iter}_{\max} \cdot I)$, which remains tractable under typical parameter settings. Fig.1 and Algorithm 3 show the overall procedures of the algorithm.

IV. Simulation Results

In this section, we perform extensive simulations to evaluate the performance of our proposed algorithm.

A. Simulation Setup

During the simulation process, we used the Python to construct our software environment. The experimental parameters are determined by considering the insights and methodologies outlined in the previous works: [20], [23]. We utilize satellite tool kit (STK) to acquire latitude and longitude data for the

LEO satellites. We consider a LEO satellites constellation consisting of 20 satellite nodes with an orbital altitude of 750km. The orbit inclination is set at 58.5 degrees. Specifically, users and eavesdroppers are randomly generated within the satellite coverage area of [23.7°N–36.6°N, 94.5°E–129.1°E] during the first time slot. This coverage is formed by a constellation of 20 LEO satellites deployed over 5 adjacent orbital planes, with each plane hosting 4 satellites. The simulation window starts from 2025-07-01 04:00:00, and each time slot spans 5 seconds. We set the beamwidth of satellites to 40 degrees. We set the transmit power of satellite nodes to 5W, and the transmit and receive antenna gains are set to 12dB. The overall system noise temperature is 25dBK. The ratio of the necessary received energy per bit to the noise density is established at 9.6dB, with a designated link margin of 2500km. The available satellite bandwidth is set to 1MHz. We set different number of active legitimate users and eavesdroppers in each timeslot. Δ in the first stage is set to 0.05. The task generating size is ranging from 10MB to 20MB. The computational workload for processing each bit computing task is modeled by a uniform distribution within [300,500] CPU cycles.

The simulation is performed on the following schemes. For the various heuristic algorithms used in the second task scheduling stage, the population size is 30 and the maximum number of iterations is 200. We conducted a series of experiments to obtain accurate and reliable results. To evaluate the effectiveness of our proposed scheme, we compared it with the following baseline schemes:

- Random scheme: In the first stage, random scheme means that users associate available LEO satellite randomly. In the second stage, random schemes means that user tasks randomly schedule to LEO satellites.
- Greedy scheme: In the first stage, user choose the LEO satellite which has the minimum $\theta_{n,u}$ to associate. In the second stage, user schedules task to the nearest LEO satellite.
- Without AN scheme: In the first stage, LEO satellites do not use AN for transmission, and user associates with available LEO satellite with better $R_{n,u}^{\text{sec}}$.
- PSO scheme: In the second stage, we use particle swarm optimization (PSO) [24] algorithm to obtain the scheduling decision.
- GA scheme: In the second stage, we use genetic algorithm (GA) [25] to obtain the scheduling decision.

B. Simulation Results

The simulation results presented in Fig.2 demonstrate the effectiveness of the proposed scheme in comparison to PSO and GA algorithms. The proposed scheme exhibits superior convergence performance, achieving a more optimal cost value within approximately 200 iterations. In contrast, the PSO scheme exhibits a slower convergence rate, with the cost value stabilizing after roughly 125 iterations. The GA scheme, while showing some initial improvement, ultimately achieves a less optimal cost value than the proposed scheme. These

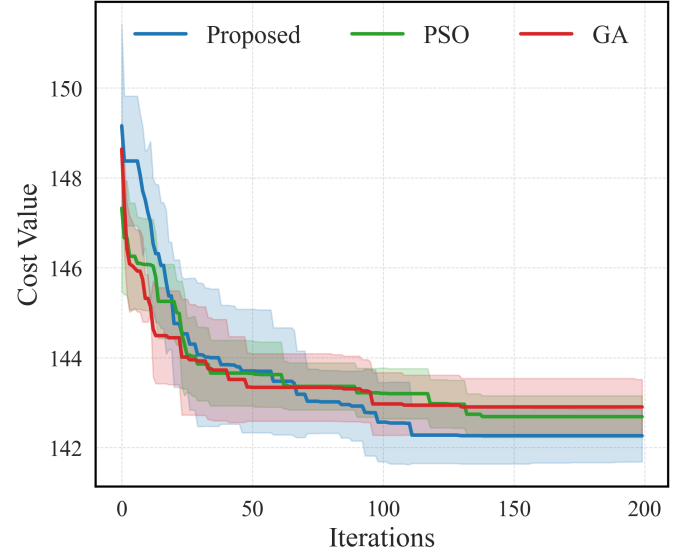


FIGURE 2. Task scheduling converge performance of different schemes.

results highlight the proposed scheme's advantages in terms of convergence speed, stability, and final solution quality, indicating its effectiveness in solving the task scheduling problem.

The radar chart in Fig.3a vividly illustrates the performance of different schemes in terms of reliable transmission rate across varying numbers of legitimate users when eavesdropper number is 5 in the first user association stage. As the number of legitimate user increases, the reliable transmission rate of all four schemes have little change due to the randomness of user position. As can be seen, our proposed scheme achieves the highest reliable transmission rate across all user counts, demonstrating its superiority in enhancing transmission security and reliability. The scheme without AN exhibits lower performance, indicating the critical role of AN in safeguarding transmissions. Due to the without AN scheme can choose LEO satellite with better R^{sec} , it can still achieve a certain level of security. Notably, the random scheme underperforms compared to the greedy scheme. This is likely because the nearest satellite typically offers better SINR for legitimate users, thereby improving the transmission quality and security. When the number of legitimate user is 30, the reliable transmission rate of the proposed scheme is reduced by approximately 77.7%, 74.5%, and 50.7% compared to the random, greedy, and without AN schemes, respectively.

The radar chart in Fig.4a provides a clear comparison of the reliable transmission rates achieved by different schemes under varying numbers of eavesdroppers when legitimate number is 30 in the first user association stage. As the number of eavesdroppers increases, the reliable transmission rate of all four schemes shows an downward trend, indicating that a larger number of eavesdroppers leads to higher security risk. It is evident that the proposed scheme consistently outperforms the other schemes across all eavesdropper counts,

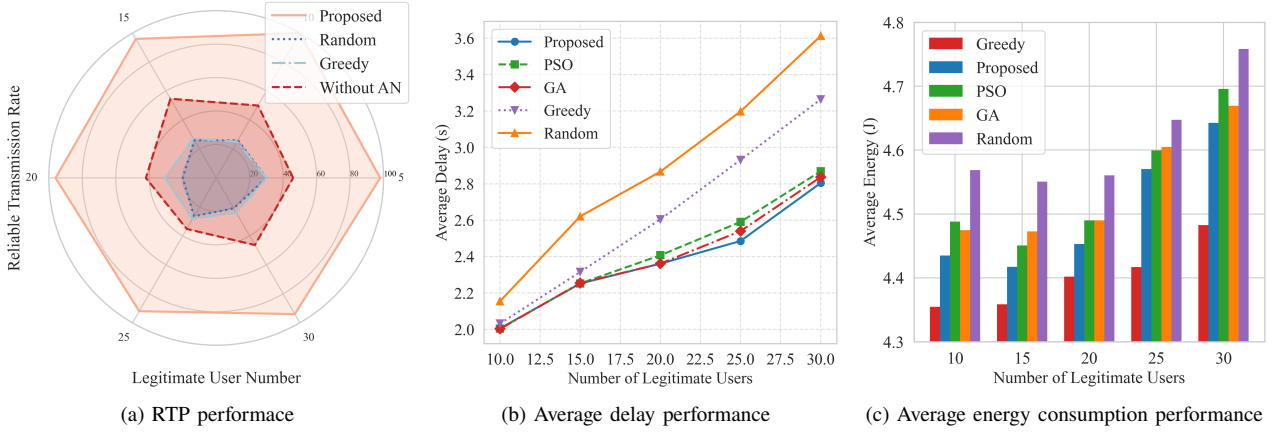


FIGURE 3. Performance of different schemes under different number of Legitimate users.

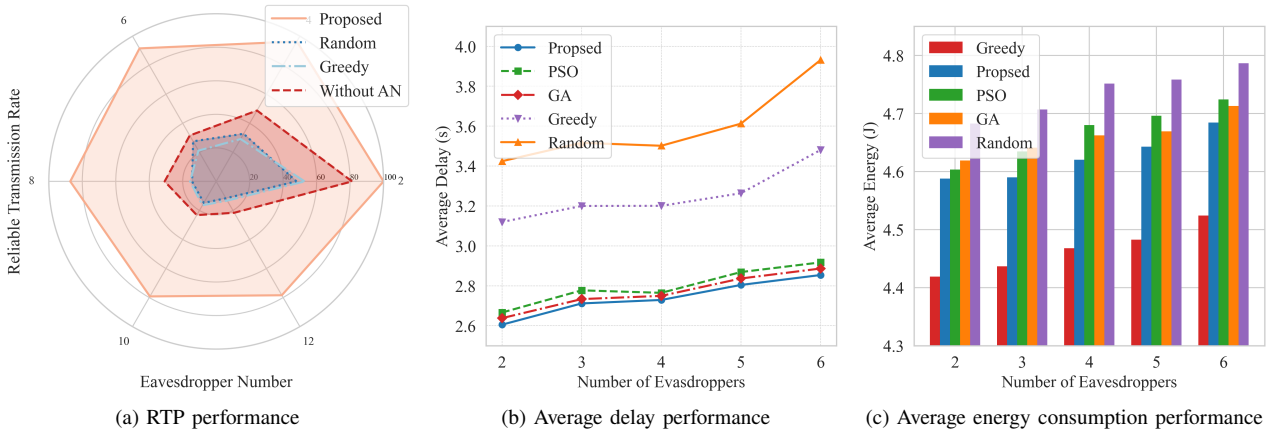


FIGURE 4. Performance of different schemes under different number of Eavesdroppers.

demonstrating its effectiveness in maintaining a high level of transmission security and reliability even in the presence of multiple eavesdroppers. The performance of without AN scheme highlights the importance of AN in protecting against eavesdropping. The results further reinforce the superiority of the proposed scheme in optimizing user association for secure communications in environments with different numbers of eavesdroppers. When the number of eavesdropper is 12, the reliable transmission rate of the proposed scheme is reduced by approximately 85.2%, 83.2%, and 72.4% compared to the random, greedy, and without AN schemes, respectively.

The simulation results presented in Fig.3b and Fig.3c provide comprehensive insights into the performance of different schemes in terms of average delay and average energy consumption as the number of legitimate users increases when eavesdropper number is 5. In Fig.3b, the delay across schemes shows an upward trend as the number of legitimate users grows, due to more user tasks will result in greater queuing delay and transmission delay. The random scheme exhibits the highest average delay. The greedy scheme also shows a notable increase in delay, though slightly less pronounced than the random scheme. Among all schemes, the proposed scheme demonstrates the lowest average delay. When the number

of legitimate user is 25, the average delay of the proposed scheme is reduced by approximately 28.5%, 18.0%, 2.2%, and 4.2% compared to the random, greedy, GA and PSO schemes, respectively.

Fig.3c illustrates the average energy consumption trends. As the number of legitimate users increases, energy consumption rises across all schemes. The random scheme consistently consumes the most energy. The greedy scheme displays the lowest energy usage, due to all the task are scheduled to the nearest LEO satellite. In contrast, the proposed scheme achieves the second lowest energy consumption, with values consistently below those of other schemes. When the number of legitimate user is 25, the average energy consumption of the proposed scheme is reduced by approximately 5.2%, 5.0%, and 4.0% compared to the random, GA and PSO schemes, respectively.

The simulation results in Fig.4b and Fig.4c offer valuable insights into how different schemes perform in terms of average delay and average energy consumption as the number of eavesdroppers increases when legitimate user number is 30. In Fig.4b, the average delay shows a little upward trend across all schemes as the number of eavesdroppers grows. This is because as more eavesdroppers emerge, users have

fewer options to stay security. The random scheme exhibits the highest average delay. The greedy scheme also shows a notable increase in delay, though it is slightly less pronounced than the random scheme. Among all schemes, the proposed scheme demonstrates the lowest average delay. When the number of eavesdroppers is 6, the average delay of the proposed scheme is reduced by approximately 37.2%, 22.0%, 1.2%, and 1.9% compared to the random, greedy, GA and PSO schemes, respectively.

Fig.4c illustrates the average energy consumption trends. As the number of eavesdroppers increases, energy consumption rises across all schemes. The random scheme consistently consumes the most energy. The greedy scheme still displays the lowest energy usage due to nearest scheduling decision. The proposed scheme achieves the second lowest energy consumption, with values consistently below those of other three schemes. When the number of eavesdroppers is 6, the average energy consumption of the proposed scheme is reduced by approximately 2.6%, 0.8%, and 1.1% compared to the random, GA and PSO schemes, respectively. The delay and energy consumption change little because simply adding eavesdroppers has little impact on user task processing, and the number of users is not increased.

V. CONCLUSION

In this paper, we investigated the secure task scheduling problem in STECN under delay, energy, and physical-layer security considerations. To tackle the challenges posed by dynamic satellite topologies and resource constraints, we proposed a two-stage heuristic framework that jointly optimizes AN power allocation, user association, and task scheduling. The first stage constructs secure communication topologies by maximizing the number of users satisfying the secrecy rate constraint, while the second stage employs a mayfly algorithm to minimize delay and energy consumption under feasible associations. Simulation results demonstrate the effectiveness of our framework. Future work will explore adaptive learning-based strategies for real-time secure scheduling in larger-scale satellite constellations.

REFERENCES

- [1] B. Di, L. Song, Y. Li and H. V. Poor, "Ultra-dense LEO: Integration of satellite access networks into 5G and beyond," *IEEE Wireless Commun.*, vol. 26, no. 2, pp. 62-69, Apr. 2019.
- [2] R. M. Ferre et al., "Is LEO-based positioning with mega-constellations the answer for future equal access localization?," *IEEE Commun. Mag.*, vol. 60, no. 6, pp. 40-46, Jun. 2022.
- [3] D. Jiang et al., "QoE-aware efficient content distribution scheme for satellite-terrestrial networks," *IEEE Trans. Mobile Comput.*, vol. 22, no. 1, pp. 443-458, Jan. 2023.
- [4] R. Xie, Q. Tang, Q. Wang, X. Liu, F. R. Yu and T. Huang, "Satellite-terrestrial integrated edge computing networks: Architecture challenges and open issues," *IEEE Netw.*, vol. 34, no. 3, pp. 224-231, Jun. 2020.
- [5] H. H. Esmat, B. Lorenzo and W. Shi, "Toward Resilient Network Slicing for Satellite-Terrestrial Edge Computing IoT," *IEEE Internet Things J.*, vol. 10, no. 16, pp. 14621-14645, 15 Aug. 2023.
- [6] T. Huang, Z. Fang, Q. Tang, R. Xie, T. Chen and F. R. Yu, "Dual-Timescales Optimization of Task Scheduling and Resource Slicing in Satellite-Terrestrial Edge Computing Networks," *IEEE Trans. Mobile Comput.*, vol. 23, no. 12, pp. 14111-14126, Dec. 2024.
- [7] F. Wei, Y. Wang, G. Feng and S. Qin, "Network-Slicing-Enabled Computation Offloading in Satellite-Terrestrial Edge Computing Networks: A Bi-Level Game Approach," *IEEE Internet Things J.*, vol. 12, no. 11, pp. 16282-16297, 1 June 2025.
- [8] Y. Gao, Z. Yan, K. Zhao, T. de Cola and W. Li, "Joint Optimization of Server and Service Selection in Satellite-Terrestrial Integrated Edge Computing Networks," *IEEE Trans. Veh. Technol.*, vol. 73, no. 2, pp. 2740-2754, Feb. 2024.
- [9] Y. Xiao, J. Liu, Y. Shen, X. Jiang and N. Shiratori, "Secure Communication in Non-Geostationary Orbit Satellite Systems: A Physical Layer Security Perspective," in *IEEE Access*, vol. 7, pp. 3371-3382, 2019.
- [10] M. Shafi, "5G: A tutorial overview of standards, trials, challenges, deployment, and practice," *IEEE J. Sel. Areas Commun.*, vol. 35, no. 6, pp. 1201-1221, Jun. 2017.
- [11] Z. Han, C. Xu, G. Zhao, S. Wang, K. Cheng and S. Yu, "Time-varying topology model for dynamic routing in LEO satellite constellation networks," *IEEE Trans. Veh. Technol.*, vol. 72, no. 3, pp. 3440-3454, Mar. 2023.
- [12] X. Hu et al., "Multi-agent deep reinforcement learning-based flexible satellite payload for mobile terminals," *IEEE Trans. Veh. Technol.*, vol. 69, no. 9, pp. 9849-9865, Sep. 2020.
- [13] H. H. Esmat, B. Lorenzo, and J. Liu, "LEONS: Multi-domain network slicing configuration and orchestration for satellite-terrestrial edge computing networks," in *Proc. IEEE Int. Conf. Commun.*, 2023, pp. 6294-6300.
- [14] M. Wu, K. Li, L. Qian, Y. Wu and I. Lee, "Secure Computation Offloading and Service Caching in Mobile Edge Computing Networks," *IEEE Commun. Lett.*, vol. 28, no. 2, pp. 432-436, Feb. 2024.
- [15] T. Zhou, B. Wang, D. Qin, X. Nie, N. Jiang and C. Li, "Secure Collaborative Computation Offloading and Resource Allocation in Cache-Assisted Ultradense IoT Networks With Multislope Channels," *IEEE Internet Things J.*, vol. 12, no. 11, pp. 17828-17843, 1 June 2025.
- [16] M. I. A. Zahed, I. Ahmad, D. Habibi and Q. V. Phung, "Green and Secure Computation Offloading for Cache-Enabled IoT Networks," *IEEE Access*, vol. 8, pp. 63840-63855, 2020.
- [17] A. Talgat, R. Wang, M. A. Kishk and M. -S. Alouini, "Enhancing Physical-Layer Security in LEO Satellite-Enabled IoT Network Communications," *IEEE Internet Things J.*, vol. 11, no. 20, pp. 33967-33979, 15 Oct. 2024.
- [18] D.-H. Jung, J.-G. Ryu, W.-J. Byun, and J. Choi, "Performance analysis of satellite communication system under the shadowed-Rician fading: A stochastic geometry approach," *IEEE Trans. Commun.*, vol. 70, no. 4, pp. 2707-2721, Apr. 2022.
- [19] M. Rodríguez-Pérez, S. Herrería-Alonso, A. Suárez-Gonzalez, J. C. López-Ardao and R. Rodríguez-Rubio, "Cache Placement in an NDN-Based LEO Satellite Network Constellation," *IEEE Trans. Aerosp. Electron. Syst.*, vol. 59, no. 4, pp. 3579-3587, Aug. 2023.
- [20] D. Zhou, M. Sheng, R. Liu, Y. Wang, and J. Li, "Channel-aware mission scheduling in broadband data relay satellite networks," *IEEE J. Sel. Areas Commun.*, vol. 36, no. 5, pp. 1052-1064, 2018.
- [21] M. Merluzzi, N. D. Pietro, P. Di Lorenzo, E. C. Strinati, and S. Barbarossa, "Discontinuous computation offloading for energy-efficient mobile edge computing," *IEEE Trans. Green Commun. Netw.*, vol. 6, no. 2, pp. 1242-1257, Jun. 2022.
- [22] K. Zervoudakis, S. Tsafarakis, "A mayfly optimization algorithm," *Comput. & Ind. Eng.*, 145, 106559.
- [23] Q. Tang et al., "Joint service deployment and task scheduling for satellite edge computing: A two-timescale hierarchical approach," *IEEE J. Sel. Areas Commun.*, vol. 42, no. 5, pp. 1063-1079, May 2024.
- [24] F. Marini and B. Walczak, "Particle swarm optimization (pso). a tutorial," *Chemometrics and Intelligent Laboratory Systems*, vol. 149, pp.153-165, 2015.
- [25] C. Reeves, and J. E. Rowe, "Genetic algorithms: principles and perspectives: a guide to GA theory" *Springer Science & Business Media*, vol. 20, 2002.